Acceleration Effects in Crystal Filters-A Tutorial

R. C. Smythe

Abstract-The quasi-static method for the analysis of vibration-induced modulation in crystal filters is briefly reviewed, and a dynamic method, in which the filter is treated as a linear network with time-varying elements, is introduced. The dynamic method, which allows determination of both amplitude and phase modulation due to vibration, is illustrated by examples. It is then applied to the analysis of the spectrum clean-up case, consisting of a frequency source with an output filter, both of which are undergoing the same acceleration.

I. Introduction

UNDER VIBRATION, a crystal filter modulates signals passing through it, adding its own vibration-induced sidebands to those of the signals it passes. Both amplitude and phase modulation may occur. After briefly reviewing the quasi-static method, this paper presents a dynamic method for analyzing vibration-induced modulation in crystal filters, in which the filter is treated as a time-varying linear network. The dynamic analysis is then applied to the spectrum clean-up case in which a frequency source, such as a crystal oscillator, is followed by an output filter.

It is assumed throughout that the modulation is due entirely to the vibration-induced frequency variation of the crystal resonators, but the approach can readily be extended to include other components. Also, while the discussion is restricted to bandpass filters, the method of analysis is also applicable to bandstop filters, and to filters other than quartz crystal filters.

A. Resonator G-Sensitivity

The acceleration sensitivity of quartz crystal resonators and oscillators has recently been reviewed by Filler [1], [2]. For accelerations that are not too large, the instantaneous circular frequency, $\omega_s(\vec{a})$, of a resonator subjected to an acceleration, $\vec{a}$ = Z(t), is

$$\omega_s(\vec{a}) = \omega_s\left(1 + \vec{\Gamma} \cdot \vec{a}\right) \tag{1}$$

where $\vec{\Gamma}$ is the acceleration-sensitivity vector of the resonator and ω_s is its zero-acceleration frequency. For sinusoidal vibration:

$$\vec{a} = \vec{A}\cos\omega_v t \tag{2}$$

$$\omega_s(t) = \omega_s + \mathrm{Aw},\ \cos\omega_v t \tag{3}$$

Manuscript received July 4, 1991; revised November 1, 1991; accepted November 8, 1991.

The author is with Piezo Technology Inc. Box 547859, Orlando, FL 32854-7859.

IEEE Log Number 9200165.

where

$$\Delta\omega_s/\omega_s = \vec{\Gamma}\cdot \mathrm{a}'. \tag{4}$$

B. Quasi-Static Analysis

Before developing the dynamic method of analysis that is our principal subject, we first review the quasi-static method. Although a filter under vibration is a time-varying linear system, at vibration frequencies that are sufficiently small, the vibration-induced modulation can be estimated from a quasi-static analysis [3]. Quasi-static analysis of a filter assumes that the element values are varying sufficiently slowly that the filter response at each instant is well-approximated by the steady-state response that would be obtained if the instantaneous element values were time-invariant. The principal advantage of quasi-static analysis is its ease of use. The principal disadvantage is that it does not provide an estimate of the error arising from the quasi-static assumption.

Consider first the simplest situation, in which all the resonators of a multiresonator filter have identical acceleration sensitivity vectors, identically oriented, so that their vibration-induced frequency changes are equal. In the case of static acceleration, a constant acceleration produces a simple translation in frequency of the steady-state filter response. If we postulate a very low-frequency sinusoidal vibration, the filter response can be thought of as oscillating back and forth along the frequency axis at the vibration frequency. That is, the filter center frequency ω_o, varies according to (3), with ω_o replacing ω_s. The effect on a sinusoidal signal of frequency w is then well-approximated by its first-order change in phase and amplitude:

$$\Delta\phi_v = \Delta\omega_o(d\theta/d\omega) \tag{5a}$$

and

$$\Delta V_v = \Delta\omega_o(dG/d\omega) \tag{5b}$$

where ϕ and V are the phase and amplitude of the signal, and θ and G are the phase shift and gain of the filter.

For signals in the passband, $dG/d\omega$ is usually small enough to be neglected, so that the principal effect of vibration is phase modulation in accordance with (5a). Now, $d\theta/d\omega$ is just the negative of the group delay, $Tg(\omega)$. Hence, for sinusoidal vibration the peak deviation is

$$\phi_v = \left(\vec{\Gamma}\ .\ \vec{A}\right)\omega_o Tg(\omega_o). \tag{6}$$

A simple example will illustrate the use of the quasi-static method. Consider a two-pole Butterworth filter, with

$$|\vec{\Gamma}| = 1 \cdot 10^{-9} G^{-1}$$
$$f_o = 10 \text{ MHz}$$
$$\text{BW}_3 = 1 \text{ kHz}$$

where BW_3 is the 3-dB bandwidth of the filter. At center frequency the group delay is given by

$$Tg(\omega_o) = \sqrt{2}/\pi \text{BW}_3 = 0.45 \text{ ms}.$$

Then for a 5-G peak acceleration, the peak phase deviation is

$$\phi_v = 1 \cdot 10^{-9} \cdot 2\pi \cdot 10^7 \cdot 5 \cdot 0.45 \cdot 10^{-3}$$
$$= 1.414 \cdot 10^{-4} \text{ rad}$$

which corresponds to a single-sideband phase modulation $\mathcal{L}$ of -83 dBc. At center frequency, $dG/d\omega = 0$, so that only phase modulation is present. Note that as a result of the quasi-static assumption, these results are independent of the vibration frequency (within the limits of that assumption.)

The simplicity of the foregoing analysis is partly a consequence of assuming that all the resonators have the same G-sensitivity. When this is not the case, a quasi-static analysis can still be carried out using network sensitivities-the effect on the filter gain and phase shift of small changes in individual resonator frequencies-but considerably more computation will be required.

Because of its simplicity, the quasi-static view is quite useful where valid. However, this is not always the case. A case of particular importance is the class of spectrum clean-up filters, or post-filters, discussed in a later section, in which the vibration frequencies may exceed the filter half-bandwidth. Here the quasi-static method is clearly inadequate.

C. Dynamic Analysis

To overcome the limitations of the quasi-static assumption, the filter must be considered as a linear network with time-varying elements. As for many time-varying linear systems, the steady-state solution can be obtained, after some preliminaries, by essentially frequency-domain methods.

Consider a resonator whose equivalent circuit is given by Fig. l(a). For present purposes Fig. l(a) represents the motional impedance of a quartz crystal resonator subjected to vibration; however, it could equally-well represent many other types of resonator. If its resonance frequency varies sinusoidally, as in (3), small frequency variations can be accurately represented by a sinusoidal variation of either capacitance C or inductance *L*. Arbitrarily choosing the latter:

$$L(t) = L_0 + 2L_1 \cos \omega_v t \tag{7}$$

where

$$L_1 = (-\Delta\omega_s/\omega_s) L_0. \tag{8}$$

Substituting (4) in (8):

$$L_1 = \left(-\vec{\Gamma} \cdot \vec{A}\right) L_0. \tag{9}$$

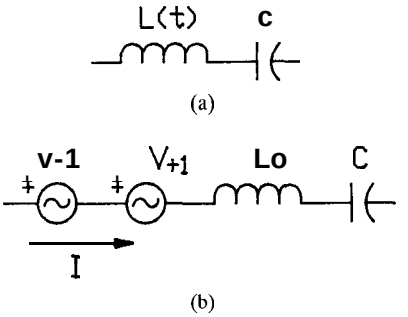

Fig. 1. Equivalent circuit of a resonator whose frequency is perturbed due to vibration. (a) Variation of resonance frequency is represented by L(t). (b) Small variations of resonance frequency can be represented by controlled voltage sources.

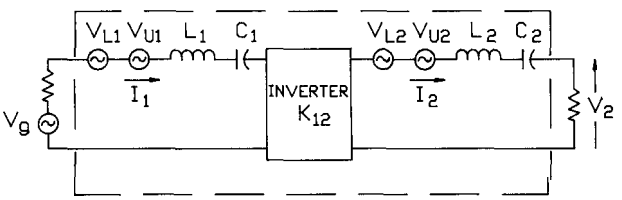

Fig. 2. Two-pole filter equivalent circuit.

It is shown in the Appendix that the effect of L_1 can be represented by a set of equivalent controlled voltage sources, one for each sideband. For the small perturbations usually of interest it is adequate to include only the first upper and first lower sidebands, as shown in Fig. l(b); however, the method is general.

To illustrate, we again consider the two-pole Butterworth filter. The coupled-resonator equivalent network of Fig. 2, which can represent several physical realizations, both discrete-crystal and monolithic, will be used. In series with each motional arm are two controlled voltage sources, one for the lower sideband and one for the upper sideband. As outlined in the Appendix, the network is first analyzed at the carrier frequency, obtaining not only the output voltage, but also the carrier frequency currents in each resonator, which are needed to determine the amplitude and phase of the sideband generators. Once the controlled-source parameters have been determined, they can be used either simultaneously, or, since superposition applies, individually to calculate the output at each sideband frequency. Finally, carrier and sideband phasors are added together at the filter output and then demodulated to separate the amplitude- and phase-modulation components.

The generality of this procedure makes it straightforward to consider cases in which the highest vibration frequency is not restricted by the quasi-static assumption. In addition, the resonators need not have identical G-sensitivities, and the relative contribution of each resonator is readily determined. All of these situations are easily handled once the analysis has been set up.

Fig. 3 plots the single sideband power as a function of the vibration frequency when both resonators have the same acceleration sensitivity. The quantities in Figs. 3, 4, and 6-9 are normalized as follows: vibration frequency is normalized by one-half the 3-dB bandwidth of the filter, BW/2; single

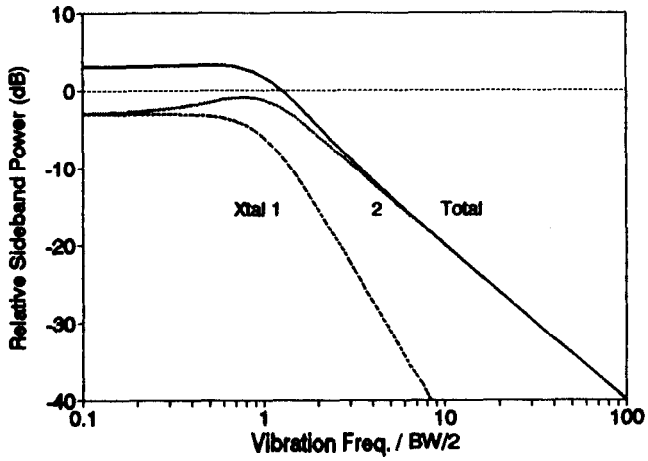

Fig. 3. Vibration-induced sideband power (normalized) for a two-pole Butterworth filter with $\vec{\Gamma}_1 = \vec{\Gamma}_2$, showing the relative contributions of the two resonators when the carrier is at band center.

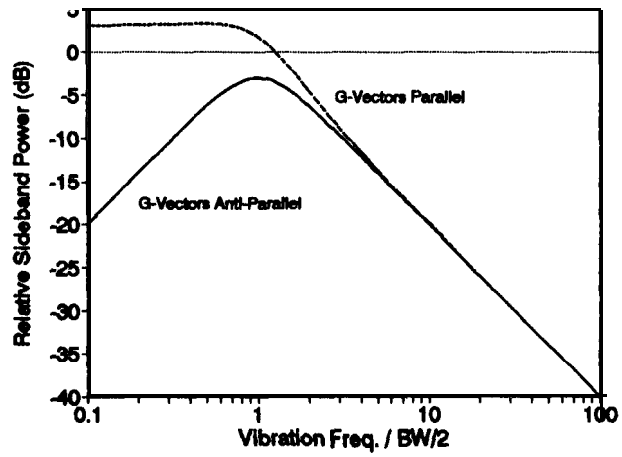

Fig. 4. Vibration-induced sideband power (normalized) for a two-pole Butterworth filter with $\vec{\Gamma}_1$ and $\vec{\Gamma}_2$ parallel and antiparallel.

sideband power is normalized by $[P_c(\vec{\Gamma} \cdot \vec{A} \cdot \omega_0/\mathrm{BW})^2]$, where P_c is the carrier power.

In Fig. 3 the carrier is at band center; hence, upper and lower sideband levels are equal. At low frequencies the level corresponds to that given by quasi-static analysis. Also shown are the sideband levels due to each resonator. As would be expected from quasi-static theory, for low frequencies the two resonators contribute equally. However, for vibration frequencies in the filter stopband, the principal contributor is resonator 2, since it is connected directly to the load, while the sidebands generated by resonator 1 are attenuated by resonator 2. Since the Butterworth transmission characteristic is symmetric, and the carrier is at the filter center frequency, there is no amplitude modulation at ω_v, although there are small AM components at even multiples of ω_v; therefore, the sideband levels plotted in Fig. 3 are entirely due to phase modulation.

It can be seen from Fig. 3 that if the two resonator G-sensitivity vectors are equal in magnitude and oriented antiparallel, then at $\omega_v = 0$ their contributions exactly cancel, as shown in Fig. 4. For high vibration frequencies, no cancellation takes place, since the output modulation is due almost entirely to resonator 2. While resonators having identical sensitivity vectors are not easily come by at the present state of the art, it is nevertheless useful to understand the basic effects.

When the carrier does not lie at band center, the vibration induces both amplitude and phase modulation. Fig. 5 shows the relative AM and PM levels as a function of carrier offset from band center, when the vibration frequency is BW/4. For small offsets, the modulation is principally phase modulation, while at large offsets it is principally amplitude modulation, the crossover occurring near $(\omega_c - \omega_o) = \pm 1.4 \cdot \mathrm{BW}/2$. Modulation is plotted in normalized form: the normalized phase modulation is $\phi_{\mathrm{peak}}/(\vec{\Gamma} \cdot \vec{A} \cdot \omega_o/\mathrm{BW})$, where ϕ_{peak} is the peak phase deviation; the normalized amplitude modulation is $m_{\mathrm{am}}/(\vec{\Gamma} \cdot \vec{A} \cdot \omega_o/\mathrm{BW})$, where m_{am} is the modulation index.

Fig. 6 compares the vibration-induced sideband levels for 2-, 4-, and 6-pole Butterworth filters in which all resonators have the same g-sensitivity and the carrier is at band center.

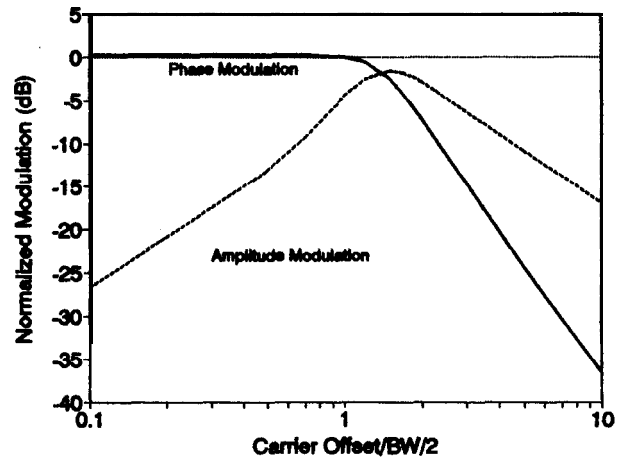

Fig. 5. Amplitude and phase modulation as a function of carrier offset for a two-pole Butterworth filter with $\vec{\Gamma}_1 = \Gamma_2$.

The coupled-resonator equivalent circuit model is used in all cases. At low vibration frequencies, the filters have the sideband levels predicted by the quasi-static model, while at high vibration frequencies, all three filters have asymptotically identical sideband levels. In this region the sidebands are due almost entirely due to the resonator nearest the load.

Because all resonators are assumed to have the same g-sensitivity, the results in Fig. 6, although obtained for filters having the coupled-resonator topology, apply for other topologies as well. The relative contributions of individual resonators to the filter's vibration performance are, however, topology-dependent.

D. Spectrum Clean-Up Filters

Many frequency sources, including both oscillators and synthesizers, use spectrum clean-up filters to reduce various spurious output components, and to lower noise floors. Spectrum clean-up filters, or post-filters, are also sometimes considered as a means of reducing vibration-induced sideband levels in a frequency source. Therefore, we now consider a frequency source whose nominally sinusoidal output is

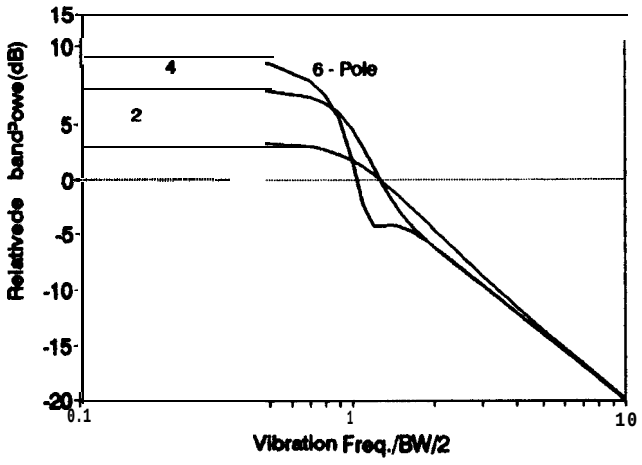

Fig. 6. Comparison of normalized vibration-induced sideband power for 2-, 4-, and 6-pole Butterworth filters. Carrier is at band center, and all resonators have the same $\vec{\Gamma}$.

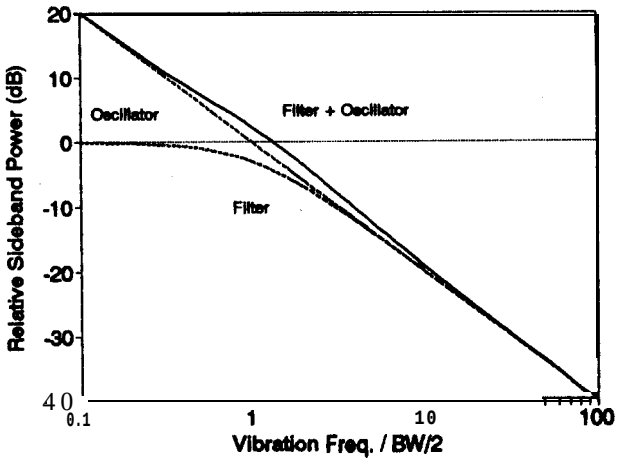

Fig. 7. Relative sideband levels for an oscillator with and without a one-pole post-filter when the filter resonator has the same acceleration sensitivity as the oscillator.

frequency-modulated due to vibration and then passed through a filter that is also subject to vibration. (The two vibration environments will be assumed to be the same, although this is not necessarily the case; e.g., if either the source or the filter is protected by vibration isolators.) The- filter in turn modulates both the carrier and the vibration sidebands of the source; however, modulation of the latter, being a second-order effect, will be neglected. Hence, the vibration sidebands of the filter output are essentially the vector sum of the sidebands of the source, attenuated and phase-shifted by the filter, and the sidebands due to the modulation of the carrier by the filter.

Since clean-up filters are ordinarily as narrow as possible, quasi-static methods may not be applicable. This was shown for a single-resonator (one-pole) filter by Horton and Morley [4] who observed that for sinusoidal vibration at frequency f_v, (3), and a sinusoidal input at a carrier frequency f_c the output is a phase-modulated signal for which, for small phase deviation:

$$\mathcal{L}(f_v) = 20\log\left(\vec{\Gamma}\cdot\vec{A}\cdot Q_L/\left[1+(2Q_L f_v/f_c)^2\right]^{1/2}\right) \quad (10)$$

where Q_L is the loaded Q of the resonator. The dynamic analysis method confirms this result. Since the 3-dB bandwidth of a one-pole filter is

$$\mathrm{BW} = f_c/Q_L. \quad (11)$$

Equation (10) can be written

$$\mathcal{L}(f_v) = 20\log\left(\vec{\Gamma}\cdot\vec{A}\cdot(f_c/\mathrm{BW})/\left[1+(f_v/\mathrm{BW}/2)^2\right]^{1/2}\right). \quad (12)$$

From (10) and (12) it can be seen that the phase modulation exhibits a frequency dependence corresponding to a one-pole filter gain characteristic. For vibration frequencies within the filter passband, the denominator in (12) is approximately 1 and the vibration-induced phase noise is nearly constant at the level predicted by quasi-static analysis. On the other hand, for vibration frequencies far removed from the passband, (10) and (12) are asymptotic to the expression [1] for the single-sideband level for a frequency source having the same acceleration sensitivity vector:

$$\mathcal{L}(f_v) = 20\log\left(\vec{\Gamma}\cdot\vec{A}\cdot f_c/2f_v\right). \quad (13)$$

Thus, at low vibration frequencies the filter's contribution to vibration-induced phase noise is less than that of a crystal oscillator using the same resonator (or, in general, any frequency source having the same acceleration sensitivity) while at high vibration frequencies the two contributions are the same. This is illustrated in Fig. 7. The curve labeled "filter" represents the phase modulation of a sinusoidal carrier by the filter; "oscillator," the phase modulation present on the unfiltered oscillator output; and "filter t oscillator" the phase modulation at the filter output, discussed below. The vibration frequency is normalized to one-half the 3-dB bandwidth, BW, of the filter; the sideband levels are shown relative to the unfiltered oscillator sideband level at BW/2.

The curve labeled "Filter+Oscillator" represents the vector sum of the sidebands of the source, attenuated and phase-shifted by the filter, and the sidebands added by the filter. It can be seen that for identical gamma vectors identically oriented, the single-pole filter does not improve the output phase modulation, but rather degrades it by as much as 2.5 dB in the vicinity of the passband edges. (However, if the gamma vectors of the source and filter were oriented antiparallel instead of parallel, some improvement would occur in the same region.) For vibration frequencies much greater than or much less than BW/2, the vibration-induced sideband level is essentially unchanged by the filter. This means that the filter may still play a useful role in cleaning up spurious responses, etc., but in order to reduce the vibration-related sidebands the filter resonator's acceleration sensitivity must be less than the frequency source's.

Fig. 8 shows the sideband levels for a source with a two-pole Butterworth postfilter when the acceleration sensitivities of the two filter resonators are the same in magnitude and orientation as that of the oscillator and the center frequency of the filter equals the oscillator frequency. It is seen that the

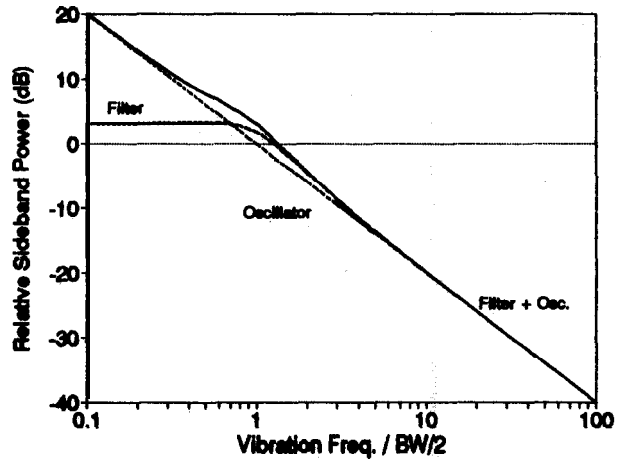

Fig. 8. Relative sideband levels for an oscillator with and without a two-pole Butterworth postfilter when the filter resonator has the same acceleration sensitivity as the oscillator.

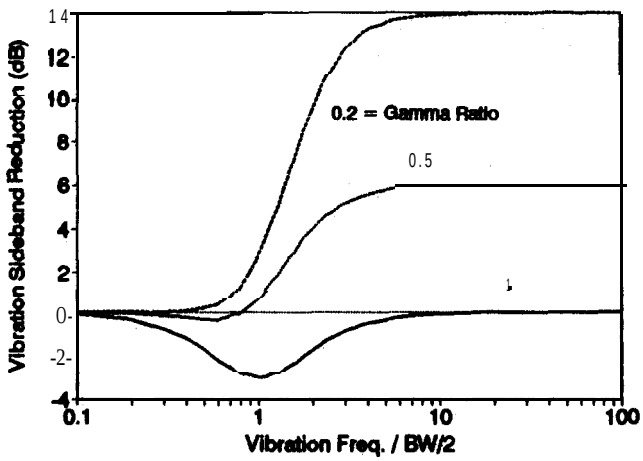

Fig. 9. Reduction in vibration sideband levels for a source with a two-pole Butterworth postfilter for three values of the gamma ratio (see text.)

filter provides no net improvement in the vibration-induced sidebands and a degradation of 3 dB at the filter passband edge. If the filter crystals are oriented antiparallel to obtain cancellation, as for Fig. 4, the only benefit in this application is to remove this 3-dB "bump."

The net effect of the filter is more easily seen in Fig. 9, which shows the vibration sideband reduction for the two-pole Butterworth as a function of normalized vibration frequency, with the gamma ratio, defined as $|\vec{\Gamma}_{\text{filter crystal}}/|\vec{\Gamma}_{\text{source}}|$, as a parameter. Three curves are shown. A gamma ratio of 1 corresponds to the equal-gamma case, Fig. 6; a ratio of 0.5, to the case in which the acceleration sensitivity of the filter crystals is one-half that of the source; and a ratio of 0.2 to the case in which the acceleration sensitivity of the filter crystals is one-fifth that of the source.

II. Conclusion

Acceleration effects in bandpass crystal filters have been analyzed by treating the filter as a linear, time-varying network, thereby overcoming the limitations of the quasi-static model. By using controlled-voltage sources to represent the vibration-induced frequency variation of the crystal resonators, the problem is reduced to the analysis of a linear network with constant coefficients. With this approach, not only can sideband levels be accurately calculated, but also, by demodulating the calculated filter output, amplitude modulation and phase modulation effects can be separately determined.

Using this method of analysis, the use of spectrum clean-up filters for improving the vibration-induced sideband level of frequency sources has been examined and found to be of limited value.

While the entire discussion has been in terms of sinusoidal vibration, because of linearity the methods apply directly to multifrequency and random vibration. Further, the method of analysis presented is not limited to crystal filters, but can be applied to any filter that can be represented by a lumped-element equivalent circuit.

Appendix
Circuit Representation and Analysis

For a linear network excited by a sinusoidal source whose frequency is ω_c and having one or more elements that are time-varying at a rate ω_v, it is readily apparent that the only frequencies present in the steady state are ω_c and sidebands at intervals of ω_v:

$$\omega_i = \omega_c + i \cdot \omega_v (i = \ldots, -1, 0, +1, \ldots). \tag{14}$$

Moreover, since the network is linear, superposition applies; we can therefore consider the variation of each element separately and then add up their combined effects. In this Appendix we model the sinusoidal variation of resonator frequency by a perturbation of the motional inductance. (This variation may be due to vibration, as in the present application, or to any other mechanism.) We then use Bolle's complex symbolism [6] to obtain the voltage-current relations for a sinusoidally varying inductor. In general, the relations include summations that are doubly infinite, but when the element variation is sinusoidal they conveniently simplify to a finite summation. This procedure yields an equivalent circuit in which the time-varying inductor is replaced by a fixed inductor and a voltage generator at each significant sideband frequency. While the method is quite general, we will consider only the case in which sidebands of second and higher orders can be neglected.

For a resonator whose frequency is varying sinusoidally at a rate ω_v, small frequency variations can be accurately represented by a sinusoidal inductance variation, (7). If we call $e_i = E_i \cos\omega_i t$ the voltage across L, and $i_i = I_i \cos\omega_i t$ the current through L, at frequency ω_i, then from (9) of Bolle, the voltages at, respectively, the first upper sideband, carrier, and first lower sideband frequency are

$$E_1 = j\omega_1[L_1 I_2 + L_0 I_1 + L_1 I_0] \tag{15a}$$

$$E_0 = j\omega_0[L_1 I_1 + L_0 I_0 + L_1 I_{-1}] \tag{15b}$$

$$E_{-1} = j\omega_{-1}[L_1 I_0 + L_0 I_{-1} + L_1 I_{-2}]. \tag{15c}$$

Up to this point, we have made no simplifying approximations. In (15a) and (15c), for the upper and lower sideband

voltages, we now neglect terms containing second-order sideband currents. We also neglect the terms containing first-order sideband currents in (15b). These simplifications are justified for most cases of interest. We then obtain

$$E_1 = j\omega_1[L_0 I_1 + L_1 I_0] \tag{16a}$$

$$E_0 = j\omega_0 L_0 I_0 \tag{16b}$$

$$E_{-1} = j\omega_{-1}[L_1 I_0 + L_0 I_{-1}]. \tag{16c}$$

In the first of these, E_1, the voltage across L at the upper sideband frequency, ω_1, is seen to be just the voltage drop across L_0 due to the upper sideband current, I_1, plus a voltage $V_1 = j\omega_1 L_1 I_0$. The latter can be represented by an equivalent controlled voltage source whose output is proportional to I_0; E_{-1} can be treated siniilarly, so that we obtain the equivalent circuit representation of Fig. l(b).

Using this equivalent circuit the complete network can then be analyzed as a linear network with constant coefficients using any modern linear network analysis program. The network is first analyzed at the carrier frequency with $L = L_0$, obtaining the current I_0, which allows us to calculate the equivalent generator voltage V_1. The network, excited now by this voltage generator, is analyzed at the upper sideband frequency, ω_1. This step is then repeated at the lower sideband frequency.

In this manner the contribution of each time-varying element can be calculated. For analysis programs that allow more than one generator, the total contribution of all the variable elements can be determined by a single analysis at each sideband frequency; otherwise, the effect of each element can be calculated separately, these results being combined to get the net effect.

From the network analyses, phasor representations of the carrier and each sideband of interest are obtained. These are then added together to construct the output signal, which is demodulated numerically to obtain the AM and PM components. This can be done most easily by shifting the carrier frequency to zero. If we call the frequency-shifted signal:

$$v(t) = V(t) \cdot \exp(j\phi(t)) \tag{17}$$

then the peak phase deviation is given by

$$\phi_{\text{peak}} = \{\max[\phi(t)] - \min[\phi(t)]\}/2 \tag{18}$$

and the amplitude-modulation index is given by

$$m_{am} = \{\max[V(t)] - \min[V(t)]\}/\{\max[V(t)] + \min[V(t)]\} \tag{19}$$

where the maximum and minimum are taken over one period of the lowest vibration frequency. If it is known that the output is essentially only amplitude-modulated or only phase-modulated, then the modulation index and related quantities can be obtained directly from the sideband levels relative to the carrier.

ACKNOWLEDGMENT

A portion of this paper first appeared in a report [5] by the members of Working Group 4 (Acceleration Effects) of the IEEE Standards Coordinating Committee 27 on Time and Frequency. The author wishes to thank Dr. John Vig, Chairman of the Working Group, for suggesting that this work be expanded and presented separately. The author also wishes to thank M. M. Driscoll for asking a very important question.

REFERENCES

[1] R. L. Filler, "The acceleration sensitivity of quartz crystal oscillators: A review," in *Proc. 41st Annu. Symp. Freq. Contr.*, 1987, pp. 398–408.

[2] R. L. Filler, "The acceleration sensitivity of quartz crystal oscillators: A review," *IEEE Trans. Ultrason., Ferroelec., Freq. Contr.*, vol. 23, no. 3, pp. 297-305, May, 1988.

[3] R. L. Clark and M. K. Yurtseven, "Spurious signals induced by vibration of crystal filters," in *Proc. IEEE Ultrason. Symp.*, 1988, pp. 365-368.

[4] T. S. Payne, "Improved tactical miniature crystal oscillator," First Interim Rep., SLCET-TR-86-0011-1, U.S. Army Laboratory Command, Fort Monmouth, NJ, Nov. 1987. (The section of this report that deals with the vibration sensitivity of crystal filters was prepared by W. H. Horton and P. E. Morley.)

[5] J. Vig *et* al., "The effects of acceleration on precision frequency sources," Research & Development Tech. Rpt. SLCET-TR-91-3, U.S. Army Laboratory Command, Electronics Technology and Devices Laboratory, Ft. Monmouth, New Jersey, Mar. 1991.

[6] A. P. Bolle, "Application of complex symbolism to linear variable networks," *IRE Trans. Circuit Theory*, vol. CT-2, no. 1, pp. 32-35, Mar. 1955.

Robert C. Smythe (M'58–SM'69) received the B.A. degree and the B.S. degree in electrical engineering in 1952 and 1953, respectively, from Rice University, Houston, TX, and the M.S. Eng. degree in electrical engineering from the University of Florida, Gainesville, in 1957.

Since 1965 he has been with Piezo Technology Inc., Orlando, FL, where he is Senior Vice-President, Research and Engineering. He is a member of the Acoustical Society of America and the American Association for the Advancement of Science. He received the IEEE Region 3 Outstanding Engineer Award in 1989 and the Walter G. Cady Award from the 45th Annual Symposium on Frequency Control, sponsored by the IEEE-UFFC Society, in 1991.